

## Spatial Structure and Dynamics of a Pulsed Arc Discharge in Vacuum

S. G. Davydov<sup>a</sup>, A. N. Dolgov<sup>a</sup>, M. A. Karpov<sup>a</sup>, A. V. Korneev<sup>a,\*</sup>, D. V. Nikishin<sup>a</sup>,  
A. A. Pshenichniy<sup>a</sup>, and R. Kh. Yakubov<sup>a</sup>

<sup>a</sup> All-Russia Research Institute of Automatics, Moscow, 127055 Russia

\*e-mail: korneev.andrey.555@mail.ru

Received March 20, 2019; revised March 20, 2019; accepted March 20, 2019

**Abstract**—The process of switching a short vacuum gap using an auxiliary discharge over the surface of a dielectric is studied by the high-speed recording of images of the plasma in the optical spectral range. Based on the analysis of the obtained experimental data, it is suggested that the cathode spot and cathode flame in the ultraviolet spectral range play a significant in the formation of current channel in the discharge.

**Keywords:** spark discharge, arc discharge, cathode spot

**DOI:** 10.1134/S1063780X20040017

### 1. INTRODUCTION

Spark and arc discharges in vacuum are of interest due to their successful applications in high-voltage and high-current electronics and in particular, in switching devices and devices for sputtering the materials for thin-film technologies, as well as in ion sources. Despite such a broad range of practical applications of spark and arc discharges, we cannot say that the mechanisms of generation and operation of a key element of these discharges such as the cathode spot [1–5] are understood fully. One of the widely accepted [3–5] models of the cathode spot that is currently being developed is the acton model [6, 7].

Understanding the nature of the cathode spot phenomenon will probably make the application of spark and arc discharges in different practical tasks even more successful.

The objective of this work is to conduct a series of studies to increase the efficiency of vacuum switches.

### 2. EXPERIMENTAL SETUP

The studies were carried out using an experimental stand which allows us to naturally model the switching process in a short vacuum gap using an auxiliary discharge over the surface of a dielectric. The construction of the discharge device is shown in the photograph in Fig. 1. The complete experimental setup is shown in Fig. 2.

The main elements of the electric discharge system were the anode, the cathode, the igniter electrode, and the dielectric plate that separated the cathode and the igniter electrode and was held tightly between them.

The electrodes are affixed on a dielectric frame. The cathode, the igniter electrode, and the dielectric plate are coaxial cylinders with the same diameter (6 mm). The cathode and the igniter electrode consist of current conductors and attachments that are in direct contact with the dielectric plate. The anode, which is a dome-shaped 6-mm-diameter part, becomes a current conductor that is screwed into a 7-mm-diameter base made from brass. The dielectric plate is 100 μm

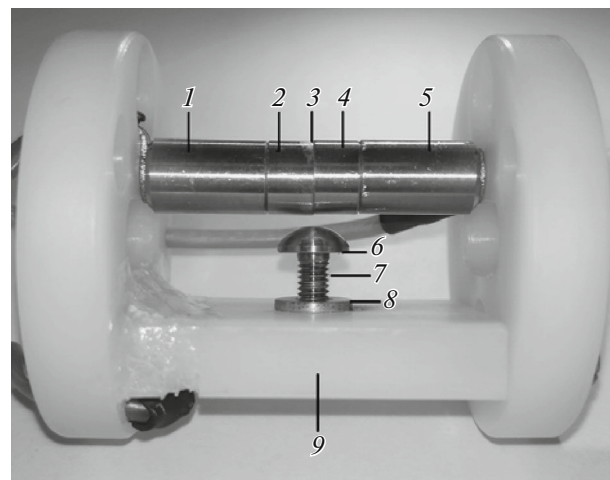


**Fig. 1.** Photograph of the vacuum diode: (1) current conductor of the cathode, (2) replaceable cathode knob, (3) dielectric plate, (4) replaceable igniter electrode knob, (5) current conductor of the igniter electrode, (6) anode, (7) current conductor of the anode, (8) anode base, and (9) dielectric frame of the vacuum diode.

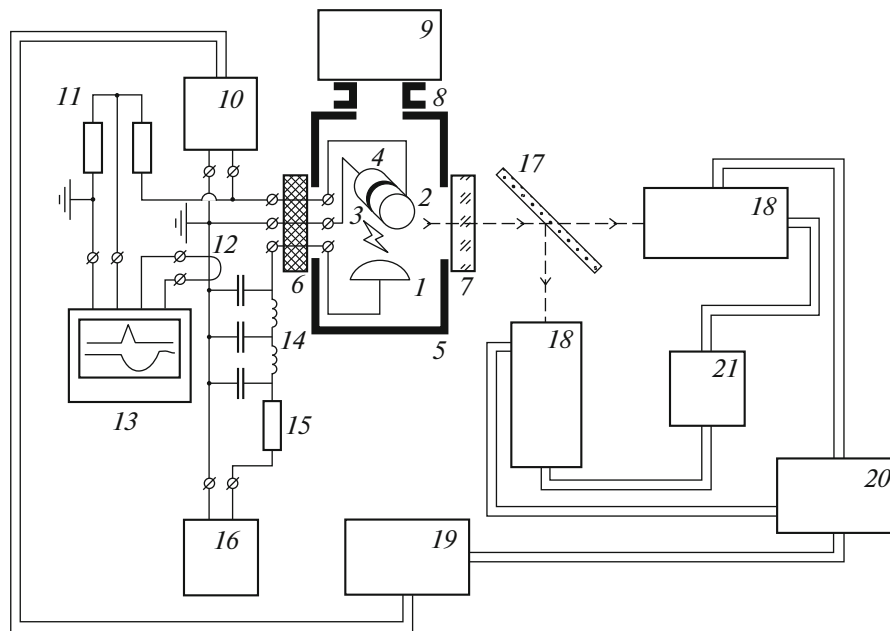


**Fig. 2.** General experimental setup: (1) anode, (2) igniter electrode, (3) dielectric plate, (4) cathode, (5) vacuum chamber, (6) flange with insulated high-voltage current conductors, (7) optical fiber, (8) vacuum tract, (9) vacuum evacuation and control system, (10) high-voltage pulse generator, (11) low-inductance Ohmic voltage divider, (12) Rogowsky coil, (13) oscilloscope, (14) forming line, (15) limiting resistance, (16) high-voltage source, (17) beamsplitter mirror, (18) image tube unit, (19) control unit of the recording channels, (20) delayed pulse generator, and (21) image storage unit.

thick. The electrodes are made from stainless steel and the dielectric plate is made from mica. The dielectric frame of the discharge device is made from Caprolon.

The discharge device is placed in a vacuum chamber that is evacuated to a residual pressure of  $10^{-2}$  Pa and is equipped with leak-proof lead-out current conductors, which allow us to connect the electric discharge device to external circuits, and an optically transparent window for extraction of the discharge plasma radiation from the chamber.

The vacuum discharge unit serves as a switch with an adjustable resistance of the LCR circuit. The cathode of the diode is grounded, while the anode has a positive voltage of up to 3 kV before switching. The commutation process starts when a positive (with respect to the cathode) voltage pulse with an amplitude up to 4 kV and rise rate of  $(1-2) \times 10^9$  V/s is applied to the igniter electrode. Thus, a discharge is ignited over the surface of the dielectric plate and the plasma of the erosion products creates the conducting medium in the cathode–anode gap. The amplitude of the ignition current reaches 10 A. The amplitude of the current in the cathode–anode gap is up to 250–300 A. The duration of the current pulse during the cathode–anode gap is determined by the parameters of the switching circuit and is about 30  $\mu$ s.

The voltage on the cathode–igniter electrode gap was recorded using a low-inductance Ohmic voltage divider. The current on the same cathode–igniter

electrode gap was determined from the voltage on the low-inductance resistance of  $10 \Omega$  connected to the igniter circuit. The current on the cathode–anode gap was determined from the signal of a calibrated Rogowsky coil.

The dynamics of the discharge in the vacuum gap was studied by recording images of the discharge plasma in its self-emission in the optical range at exposition times of 5 to 500 ns. The images were recorded by an electrooptical block that consisted of the following units:

- (i) two image tube blocks that used cathode gating scheme,
- (ii) the registration channel control unit,
- (iii) the beamsplitter mirror,
- (iv) the 4-channel DG645 delayed pulse generator used to synchronize the start of the recording channels and the igniting circuit of the spark gap, and
- (v) the image storage unit (notebook and software).

In turn, both image tubes blocks consisted of the following parts:

- (i) the strobing pulse generator (SPG) over the cathode,
- (ii) the transporting lens (Jupiter), and
- (iii) the EPM-102G image tube connected to the SDU-274 digital CCD camera with a resolution of  $1600 \times 1200$  pixels through a VEGA projection lens to record the information from its screen.

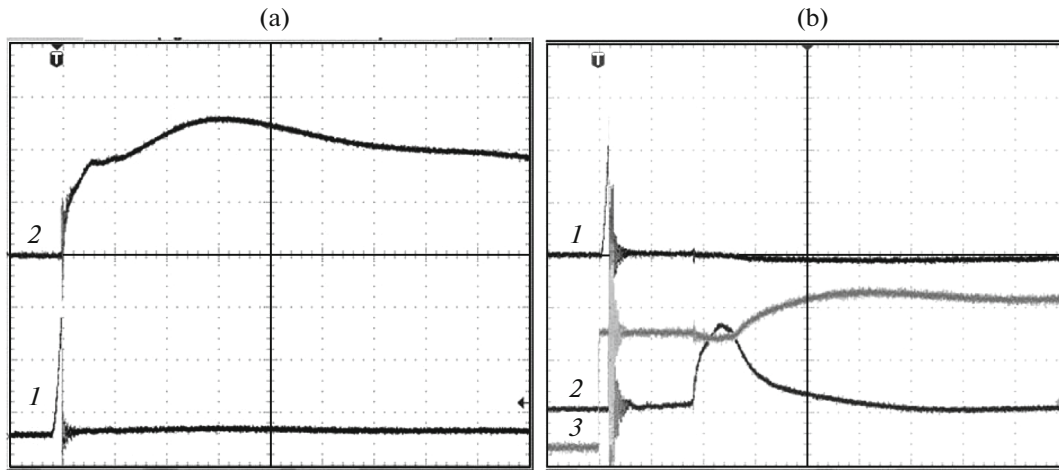


**Fig. 3.** Time dependences of the voltage on the cathode–igniter electrode gap (line 1) and the current in the cathode–anode gap (line 2). (Line 3 is the signal of the registration block control unit.) The sweep time is of  $2 \mu\text{s}/\text{division}$ . The sensitivity of line 1 is  $1 \text{ kV}/\text{division}$ , line 2 is  $100 \text{ A}/\text{division}$ , and line 3 is  $2 \text{ V}/\text{division}$ . (a) Discharge of the first type and (b) discharge of the second type.

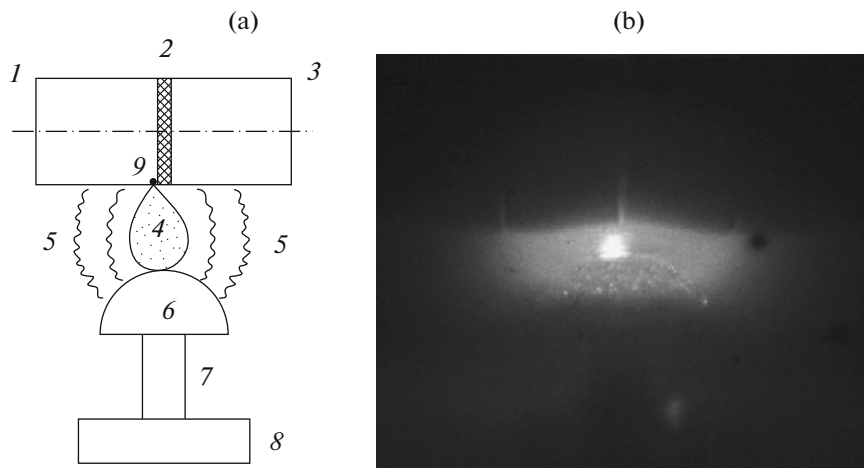


**Fig. 4.** Observed discharge of the first type. (a) Spatial structure of the discharge: (1) cathode, (2) dielectric plate, (3) igniter electrode, (4) cathode flame, (5) discharge periphery, (6) anode, (7) current conductor, (8) anode base, and (9) cathode spot; (b) discharge image in the optical radiation obtained by the high-speed photography system. Exposition: the start of the recording at  $t = 1.9 \mu\text{s}$  after the start of the current in the cathode–anode gap; the image was recorded during  $\Delta t = 0.5 \mu\text{s}$ .

To obtain two frames separated by a certain time interval that record the images of the discharge plasma in the optical wavelength range with the set exposition, the channels were placed relative to the object under study along a parallax-free trajectory with a beamsplitter mirror.

### 3. EXPERIMENTAL RESULTS AND DISCUSSION

The discharges under study can be separated into two types. Figure 3 shows the characteristic time

dependences of the voltage in the ignition system and the current in the cathode–anode gap for both discharge types.

In the first discharge type, an arc discharge develops in the cathode–anode gap; i.e., the current drift of charged particles in the conducting medium (plasma) occurs along the shortest trajectory between the cathode and the anode (see Fig. 4a). The first main discharge type is realized when the auxiliary spark discharge along the dielectric surface, which initiates the discharge between the cathode and anode, and ignites

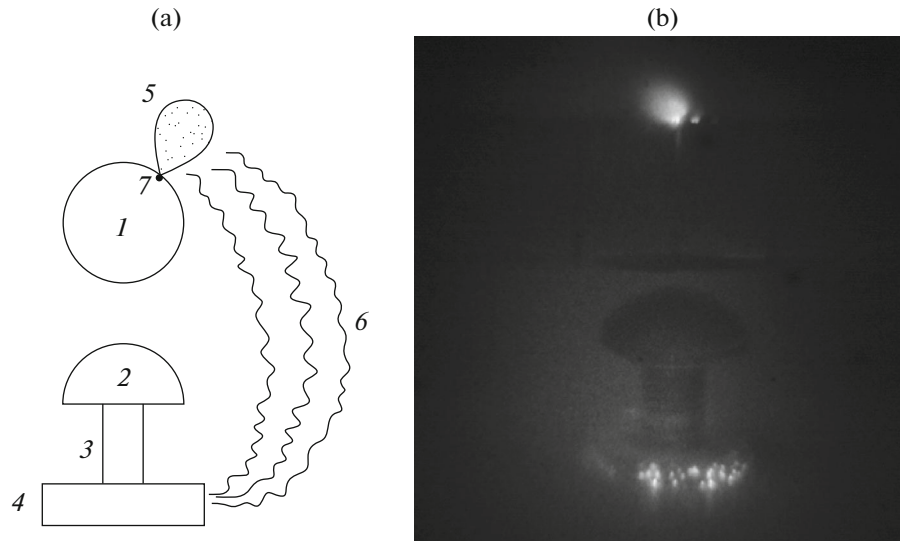


**Fig. 5.** Observed discharge of the second type. (a) Spatial structure of the discharge: (1) cathode, (2) anode, (3) current conductor, (4) anode base, (5) cathode flame, (6) discharge periphery, and (7) cathode spot; (b) discharge image in the optical radiation obtained by the high-speed photography system. Exposition: the start of the recording at  $t = 300$  ns after the start of the current in the cathode–anode gap; the image was recorded during  $\Delta t = 100$  ns.

on the area of the ignited system that is at the minimum distance from the anode surface.

Figure 4b, apparently, shows the arc stage of the discharge in the cathode–anode gap, judging from the current and the time interval during which the discharge is developing. The brightest radiation source, at least, in the optical range, is the plasma column in the cathode–anode gap. Note that the cathode spot, which is located at the base of the column on the cathode, is the center of a diffusely radiating discharge region, which has the shape of a semisphere. At the intersection of the radiating region with the anode surface, multiple sources of optical radiation (probably anode spots) with dimensions of about 0.1 mm and a layer of anode material vapor slightly elevated above the anode surface are observed.

It is probable that the ultraviolet (UV), not optical, radiation of the arc discharge causes the ionization of the rarefied gas medium at the periphery of the discharge and that a weak current flows in this rarefied medium along with the stronger current in the main strongly radiating current channel. Evidence supporting the simultaneous existence of two spatially separated discharge regions is provided by the cloud of the anode material vapor seen in the photograph and the anode spots present at the upper boundary of the vapor. In the region with a high density of matter and high current an arc discharge takes place. In the second region with a low density and low current a discharge that resembles a glow discharge takes place.

It is known that the glow discharge is subject to the thermal–ionization instability, which leads to the contraction of the current channel [8, 9]. The contrac-

tion manifests in the outer region of the discharge as the appearance of localized anode spots at the anode surface and the boundary of the vapor of the anode material.

The main discharge of the second type is realized when the auxiliary spark discharge appears at the area of the igniter system whose distance from the anode surface is close to maximum. The anode surface at a distance of 1 mm from the cathode surface in this case does not participate in the development of the discharge between the cathode and anode, and the current lines cross the surface of the anode base. The length of the trajectory of the current drift of charged particles in this case increases by more than one order of magnitude (Fig. 5a). Figure 5b, judging by the current and the duration of the discharge development, shows the spark stage of the discharge in the cathode–anode gap. At least, this occurs where the region of the discharge that can be visibly observed near the cathode and igniter electrode surface. A cathode spot and cathode flame, i.e., a plasma flow emitted from the cathode spot, are observed on the cathode surface at the boundary of the dielectric plate. An anode spot is observed at the boundary between the igniter electrode and the dielectric plate. In addition, multiple anode spots are observed at the anode base. We can discern a diffused glow in the space around the cathode and anode. At the same time, no visual signs of the discharge in the cathode–anode gap are seen.

Despite the attained discharge current and duration, the visual characteristics of the discharge of the second type are atypical at the stage that can be called the arc discharge stage (see Fig. 6). A cathode spot and



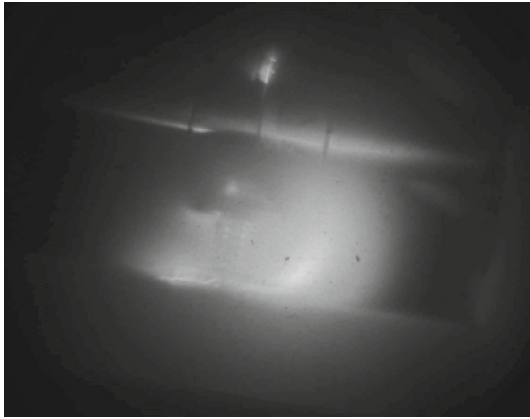


**Fig. 6.** Image of the discharge in the optical radiation obtained by the high-speed photography system. Exposition: the start of the recording at  $t = 1.9 \mu\text{s}$  after the start of the current in the cathode–anode gap; the image was recorded during  $\Delta t = 100 \text{ ns}$ .

cathode flame are observed, and often, an anode spot on the surface of the igniter electrode can also be seen. In the space around the electrode system, a diffuse glow is seen, and on top of it, a radiating band directed toward the anode base. At the same time, no discharge in the cathode–anode gap is observed and no glowing anode spots at the anode base are visible.

The second discharge type is, apparently, a mixed spatially inhomogeneous discharge, the same as the first discharge type. The discharge parameters at the cathode surface in the cathode flame, apparently, correspond to the parameters of the discharge that passes through spark and then arc stages in vacuum.

However, the characteristics of the region with the diffuse glow are different. The cathode material requires  $1\text{--}10 \mu\text{s}$  to spread from the cathode spot to the anode base. The upper boundary of this time interval corresponds to the spread of the cathode material vapor at the thermal velocity of about  $10^3 \text{ m/s}$  and the upper boundary corresponds to the propagation of the plasma of the cathode flame due to ambipolar diffusion at a velocity of about  $10^4 \text{ m/s}$ . Thus, the discharge, whose glow at the periphery of the electrode system is recorded in the photographs, begins to operate in the rarefied residual gas. Note that the vacuum conditions in the diode are such that, at the set initial voltage on the cathode–anode gap of  $3 \text{ kV}$ , there are no signs of ignition of a self-sustained glow discharge.

The second discharge type differs from the first discharge in that, first, its two current-conducting regions are connected to the electric circuit in series. Second, the contraction of the current channels in the low-density region is observed only at the initial, spark, stage of the discharge. Later, no anode spots, which can serve as proof as the contraction of the current channel, are observed at the anode base. How-

ever, the peripheral region of the discharge with, mostly, low density, still forms under the action of the radiation from the high-density region (the cathode spot and the plasma flame) near the cathode, and it is still similar to the glow discharge in its method of current channel formation. It is known that if the distance between the cathode and anode is shorter than that which is required for the appearance of a dark cathode space and the start of the glow but a longer path from the cathode to the anode can be created in the surrounding space, the glow discharge chooses this longer path to form the current channel [10].

#### 4. NUMERICAL ESTIMATES

Let us estimate the initial current that can flow in a rarefied gas, i.e., in a vacuum, in our electrode system. In the case of the discharge of the first type at voltage  $U = 3 \text{ kV}$  and distance between the electrodes, i.e., the cathode and the anode,  $\delta = 1 \text{ mm}$ , the well-known three-halves power law [11]

$$j_{3/2} = 2.33 \times 10^{-6} U^{3/2} / \delta^2 \quad (1)$$

gives a current density of about  $3 \times 10^5 \text{ A/m}^2$ . If we take the cross section of the current channel equal to  $\sim 10^{-6} \text{ m}^2$  (the current channel diameter of  $\sim 1 \text{ mm}$ ), then the total current is  $\sim 0.3 \text{ A}$ . At the current channel cross section of  $\sim 10^{-4} \text{ m}^2$  (diameter of  $\sim 1 \text{ cm}$ ), the total current is  $30 \text{ A}$ .

It was shown that under our conditions, i.e., at a residual gas pressure of  $10^{-2} \text{ Pa}$ , the UV radiation from the cathode spot can ionize the residual gas and create the conditions for a discharge that is similar to the glow discharge. It is known that, in contrast to the glow discharge, the arc discharge is characterized by a high current density of  $\geq 10^5\text{--}10^7 \text{ A/m}^2$  [11]. The necessary condition for the development of a self-sustained arc discharge is that the discharge current exceeds a certain threshold current value. For the chemical elements from the material of the electrodes, this threshold current ranges from  $1.5$  to  $6 \text{ A}$  [6]. Thus, when the majority of the anode surface is dragged into the formation of the initial discharge, the discharge can transition to the arc phase. The threshold current, judging from the recorded current raise rate in the cathode–anode gap (see Fig. 3), is reached after  $\leq 10 \text{ ns}$ , i.e., before the decay of the initiating spark discharge along the surface of the dielectric, whose duration is  $\sim 30 \text{ ns}$ .

The obtained images of the discharge indicate that the UV radiation from the cathode spot and cathode flame can create a conductive medium in the cathode–anode gap by ionizing the residual gas and thus create the conditions for including a substantial region of the anode surface in the discharge. The cathode spot appears during the initiating spark breakdown along the surface of the dielectric. Further, the physi-

cal mechanism of the discharge transition to a self-sustained arc discharge is the thermal–ionization instability of the glow discharge, which leads to a contraction or shunting of the discharge [11]. At the initial stage of the discharge, the propagation of the plasma of the cathode flame in the electrode gap alone cannot provide such a rapid current build-up as the one indicated above. Indeed, if the thermal velocity of about  $10^3$  m/s plays a decisive role, the time required for the electrode gap to close by the cathode flame plasma is  $\sim 10^{-6}$  s. The ambipolar diffusion mechanism [6] can shorten this time to  $\sim 10^{-7}$  s.

We can assume that, at the start of the discharge of the second type, a glow-type discharge develops in the rarefied gas medium at the periphery of the cathode–anode gap, in which the contraction of the current channel is observed, while in the cathode region, the discharge is of the spark type. Further, because of the increase in the density of the charge carriers due to the particle supply from the cathode flame, the discharge becomes an arc discharge, and the anode transitions to a diffused operation regime. The filling of the discharge space by the plasma from the cathode flame leads to a relatively abrupt increase in the conductivity of the current channel. Judging by the delay time, the ambipolar diffusion mechanism does not play a decisive role under these conditions, and the diffusion velocity of the cathode flame matter is determined by the thermal velocity of the ions.

Moreover, note the protracted trailing edge of the current pulse caused by the relatively slow spatial recombination in the rare plasma outside the cathode flame. The observed characteristic decay time at the trailing edge of the current pulse is about several microseconds. The most efficient mechanism of spatial recombination in the weakly ionized gases and metal vapor is the dissociative recombination [8]. In the absence of an electric field (or at a weak field, e.g., when the current passes zero), the concentration of charged particles decreases with time by the law

$$n_e = 1/(1 + \beta n_{e0}t), \quad (2)$$

where  $n_{e0}$  and  $n_e$  are the initial electron density in the plasma and the electron density at time  $t$ , and  $\beta \approx 10^{-13}$  m<sup>3</sup>/s is the coefficient of dissipative recombination [8]. The characteristic time of plasma decay is estimated as  $\tau \approx 1/\beta n_{e0}$ . If the initial concentration of charged particles outside the cathode flame is of the order of  $10^{18}$  m<sup>-3</sup> taking into account the diffusion from the flame to the surrounding space, then we can estimate the characteristic time of plasma decay in the discharge of the second type as  $10^{-5}$  s, which agrees closely with the experimental data.

Let us estimate the initial concentration of charged particles in the plasma flame for the recombination

process in a discharge of the first type by the Jüttner formula for a vacuum arc

$$n_{e0} \approx \gamma I_{\text{arc}}/r^2, \quad (3)$$

where  $\gamma \approx 10^{13}$  A<sup>-1</sup> m<sup>-1</sup> is a constant,  $I_{\text{arc}}$  is the arc current, and  $r$  is the distance from the cathode spot [12]. If we assume that  $I_{\text{arc}} \approx 10\text{--}10^2$  A (at the current decay) and  $r \approx 10^{-3}$  m (equal to the distance between the cathode and anode), we get the estimate of a characteristic time of plasma decay in the discharge of the first type of the order of  $10^{-8}$  to  $10^{-7}$  s, which, at least, does not contradict the experimental observations of the discharge of the first type.

## 5. CONCLUSIONS

In this work, the dynamics of the commutation of a short vacuum gap using an auxiliary discharge along the surface of a dielectric was studied. To this end, images of the discharge plasma were recorded in its self-radiation in the optical range at exposition times in the subnanosecond range.

The images were obtained using a two-channel electrooptical block. Each channel contained a registration unit for the strobing pulse along the photocathode of an image tube, a transporting lens, and an image tube connected to a digital CCD camera through a projection lens to record the data.

The discharges under study can be separated in two types. In the first type, arc discharges develop in the cathode–anode gap; i.e., the current drift of charged particles in the conducting medium (plasma) occurs along the shortest trajectory between the cathode and anode. Parallel to the arc discharge channel, a diffuse discharge channel is observed. The second discharge type is characterized by the generation of a cathode spot or spots on the cathode and an ejection of a cathode flame into the surrounding space, which becomes an arc-like diffuse discharge region that closes on the anode base. In this discharge, there are no visual signs that the discharge channel develops along the shortest trajectory in the cathode–anode gap.

Based on the analysis of the experimental data, we assume that the UV radiation from the cathode spot and cathode flame play a significant role in the formation of the current channel in the discharge.

## REFERENCES

1. V. E. Ptitsin, JEPT Lett. **55**, 325 (1992).
2. I. A. Zel'tser, A. S. Karabanov, and E. N. Moos, Phys. Solid State **47**, 1921 (2005).
3. S. Anders, A. Anders, and I. Brown, Rev. Sci. Instrum. **64**, 1253 (1994).
4. V. A. Ivanov, A. S. Sakharov, and M. E. Konyzhev, Usp. Prikl. Fiz. **1** (6), 697 (2014).
5. J. Jüttner, J. Phys. D: Appl. Phys. **34**, R103 (2001).

6. G. A. Mesyats, *Ectons in Vacuum Discharges: Breakdown, Spark, and Arc* (Nauka, Moscow, 2000) [in Russian].
7. G. A. Mesyats, *Pulsed Energetics and Electronics* (Nauka, Moscow, 2004) [in Russian].
8. Yu. P. Raizer, *Gas Discharge Physics* (Nauka, Moscow, 1992; Springer, Berlin, 1997).
9. E. P. Velikhov, A. S. Kovalev, and A. T. Rakhimov, *Physical Phenomena in Gas-Discharge Plasmas* (Nauka, Moscow, 1987) [in Russian].
10. N. A. Kaptsov, *Electronics* (GITTL, Moscow, 1954) [in Russian].
11. S. K. Zhdanov, V. A. Kurnaev, M. K. Romanovsky, and I. V. Tsvetkov, *Foundation of Physical Processes in Plasma and Plasma Facilities* (Moscow Eng. Phys. Inst., Moscow, 2007) [in Russian].
12. A. Anders, presented at the *Breakdown Physics Workshop* (CERN, Meyrin, 2010).  
[https://indico.cern.ch/event/75380/contributions/2089504/attachments/1049287/1495843/Anders\\_cathodicArcs2010-05-04.pdf](https://indico.cern.ch/event/75380/contributions/2089504/attachments/1049287/1495843/Anders_cathodicArcs2010-05-04.pdf).

*Translated by E. Voronova*